Materials Chemistry and Physics 124 (2010) 44–47

Contents lists available at ScienceDirect

Materials Chemistry and Physics

journal homepage: www.elsevier.com/locate/matchemphys

Materials science communication

Synthesis, structure and optical studies of inorganic–organic hybrid semiconductor, $NH_3(CH_2)_{12}NH_3PbI_4$

K. Pradeesh [a], G. Sharachandar Yadav [a], Monika Singh [b], G. Vijaya Prakash [a,*]

[a] Nanophotonics lab, Department of Physics, Indian Institute of Technology Delhi, New Delhi 110016, India
[b] Department of Chemistry, Indian Institute of Technology Delhi, New Delhi 110016, India

ARTICLE INFO

Article history:
Received 31 December 2009
Received in revised form 26 March 2010
Accepted 18 July 2010

Keywords:
Crystal structure
Chemical synthesis
Quantum wells
Optical properties

ABSTRACT

Synthesis, crystal structure and optical properties of two-dimensional layered inorganic–organic hybrid $NH_3(CH_2)_{12}NH_3PbI_4$ are presented. Intercalation strategy has also been used to fabricate single crystal and thin films of the same. As thin film, they are well oriented and stacked along the [1 0 0] direction with strong room-temperature excitonic absorption and emission characteristics. Exciton features were correlated with the relative inorganic network crumpling and conformation of alkylammonium chains. The structural features are compared with those of similar hybrid, $(H(CH_2)_{12}NH_3)_2PbI_4$.

1. Introduction

Self-organized inorganic–organic layered semiconductors in the form of $(RNH_3)_2PbX_4$ are considered as multiple quantum well structures where organic ammonium moieties $(RNH_3)^+$ are sandwiched between two infinitely extended inorganic semiconductor layers of $[PbX_6]^{4-}$. Because of quantum and dielectric confinement, these perovskite-type hybrids show potential in many optoelectronic applications [1]. Due to the strong room-temperature excitonic properties, a great deal of attention has been paid to the preparation and characterization of wide varieties of inorganic–organic layered perovskites [2–6]. Out of all, alkylammonium chain-based lead iodides, in the generic form of $(C_nH_{2n+1}NH_3)_2PbI_4$ are of special interest because of their diverse structural phase transitions and, as a consequence, peculiar nature of their optical properties [7–9]. In general the excitonic features are critically dependent on (1) disordered orientation of alkyl chains in the organic moiety, (2) changes in the crystal structure, (3) crumpling of inorganic layers and (4) coupling between the ammonium group attached to the organic moiety and the PbI network [10]. Recently we have demonstrated switchable excitons in one of the long chain-based lead iodide hybrid, $(H(CH_2)_{12}NH_3)_2PbI_4$ (C12PI) and exemplified their ability for new device applications [10,11].

In this letter, preparation, room-temperature crystal structure and optical properties of di-ammonium-alkyl based hybrid, $NH_3(CH_2)_{12}NH_3PbI_4$ (DDPI), are described. The titled compound has been synthesized from conventional solution chemistry techniques as well as newly developed intercalation process [12]. Structural and room-temperature exciton features have been discussed and are compared with those previously reported similar layered hybrids, particularly with C12PI [8].

2. Experimental

Single crystals of DDPI were grown by the slow evaporation technique. 0.2 mmol of lead (II) iodide (0.092 g) and $NH_2(CH_2)_{12}NH_2$ (0.04 g) were dissolved separately in 7 ml of 57% HI solution and are mixed together at 65 °C. The solution was refluxed for an hour. The resultant clear solution was cooled slowly to room temperature. Yellow plate like crystals (0.5 mm × 0.5 mm × 0.2 mm) was harvested by slow evaporation of the resultant solution. Single crystals of similar long chain based hybrid C12PI were also synthesized for comparison and the details were previously reported [11]. Similarly, we have recrystalized organic moiety (hereafter DD) of dimensions 2 mm × 2 mm × 2 mm for intercalation purpose. Single crystals suitable for single crystal X-ray diffraction analysis were selected and studied. Single crystal diffraction studies were carried out by Bruker APEX CCD diffractometer with a Mo Kα (0.71073 Å) sealed tube at 293 K. The program SMART [13] was used for collecting frames of data, indexing reflection and determination of lattice parameters, SAINT [13] for integration of the intensity of reflections and scaling. SADABS [14] was used for absorption correction and SHELXTL [15] for space group and structure determination and least-squares refinements on F^2. The lead atoms were located first and then remaining atoms were deduced from subsequent difference Fourier syntheses. The hydrogen atoms were located using geometrical constraints. All the non-hydrogen atoms were refined anisotropically. The least-squares refinement cycles on F^2 were performed until the model converged. Molecular graphics were presented by Diamond v2.1c.

Thin films of DDPI were fabricated as follows: single crystals were first dissolved in solvent DMSO, drop-casted onto a glass substrate and eventually heated

* Corresponding author. Tel.: +91 11 2659 1326; fax: +91 11 2658 1114.
E-mail address: prakash@physics.iitd.ac.in (G. Vijaya Prakash).

0254-0584/$ – see front matter © 2010 Elsevier B.V. All rights reserved.
doi:10.1016/j.matchemphys.2010.07.037

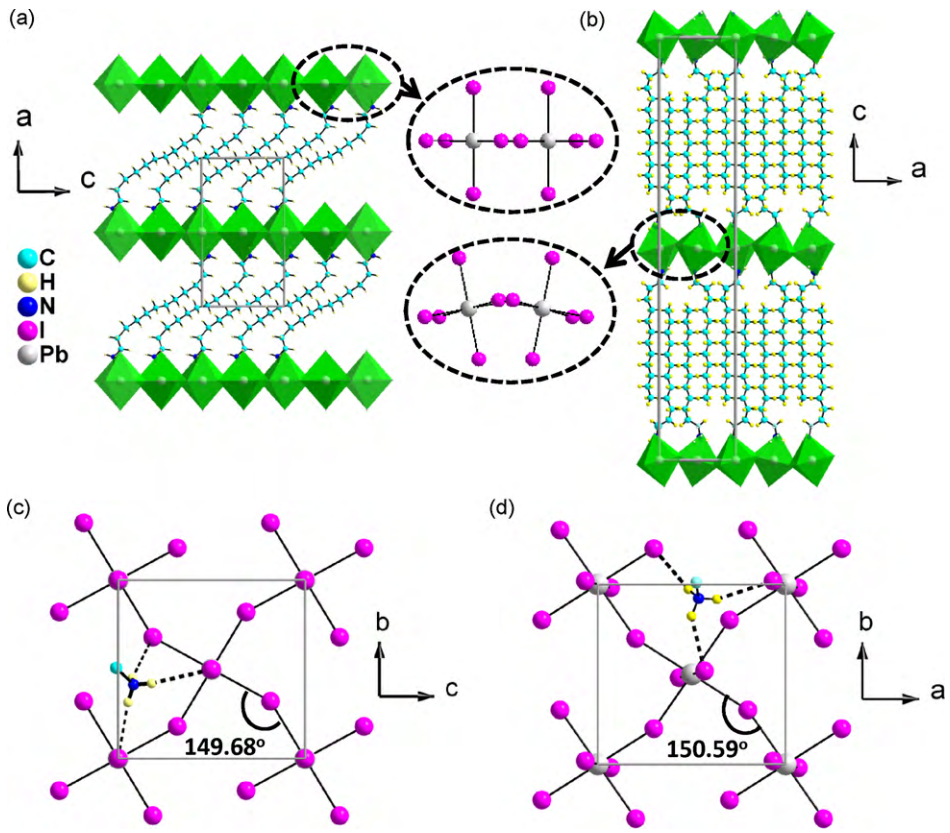

Fig. 1. 2D layered arrangement of (a) DDPI and (b) C12PI. Inset shows the respective *out-of-plane* distortion. NH-I terminal halide configurations of (c) DDPI right triangle configuration and (d) C12PI equilateral triangle configuration. The respective Pb–I–Pb bond angles are also given. Unit cell edges are shown in grey solid lines.

upto 65 °C. Once the solvent started evaporating, the substrate has been quickly transferred to a spin-coater and spun at 2000 rpm for 60 s. Uniform thin films of ~100 nm were used for glancing angle X-ray diffraction (GLAXRD) and optical studies. UV–visible absorption and photoluminescence (PL) studies were carried out using a spectrometer, white light source and 337 nm nitrogen laser. High-resolution images and PL mapping were carried out using modified confocal microscope equipped with a camera, XY direction piezo controlled sample stage, 447 nm CW diode laser and a spectrometer.

3. Results and discussion

3.1. Crystal structure

The inorganic–organic (IO) hybrid, DDPI, crystallizes as monoclinic in the space group $P2_1/c$. The asymmetric unit consists of PbI_2 anion unit and a molecule of $(NH_3(CH_2)_{12}NH_3)$ dication unit. The complete details of the crystallographic data are given in Table 1. The crystal structure features as two-dimensional layered entity with alternative stacking of inorganic and organic layers. Inorganic layers are extended as two-dimensional (2D) network by corner sharing of each distorted PbI_6 octahedra with neighboring four octahedra through the double bridging iodide. Fig. 1 compares the layered arrangement of DDPI to that of recently reported single amino-end group long chain organic moiety hybrid, C12PI.

The coordination geometry around the Pb atom shows no axial compression of the octahedral geometry. The Pb–I bond lengths range between 3.170(1) and 3.204(2) Å and the I–Pb–I *cis*-bond angles around the Pb atom, which occupies a center of symmetry, range between 87.56(3)° and 92.44(3)° while the *trans* angles are ~180°. The bridging angle Pb–I–Pb is 149.68(4)° which gives the tilt between adjacent octahedra. The Pb–I bonding nature (distance ~3.2 Å), observed here favors more towards the ionic nature (sum of ionic radii is 3.39 Å) than covalent nature (sum of covalent radii is 2.87 Å).

The di-ammonium alkyl chains occupied between the Pb–I layers are of much interest: they are much distorted from linear nature as compared to C12PI (Fig. 1a and b). The conformation of hydrocarbon as compared to its linear nature changes near to the amino groups with N–C–C bond angle 104.96(7) and C–C–C bond angle

Table 1
Crystallographic data of DDPI.

Crystal data	Dodecyl diammonium lead iodide
Empirical formula	$C_{12}H_{30}N_2PbI_4$
Formula weight	917.18 g mol^{-1}
a	16.018(3) Å
b	8.4759(19) Å
c	8.852(2) Å
Temperature	293(2) K
Radiation	Mo Kα
Diffractometer	Bruker Smart Apex CCD
Crystal system	Monoclinic
Space group	$P2_1/c$
Volume	1201.8(4) Å^3
Z	2
d_{calc}	2.535 g cm^{-3}
Crystal	Yellow
Crystal size	0.5 mm × 0.5 mm × 0.2 mm
Data collection	
No. measured reflections	4610
No. unique reflection	2214
No. observed reflections ($I > 2\sigma I$)	1212
No. refined parameters	89
R_1 ($I > 2\sigma I$)	0.0663
WR_2 (all)	0.1618
Min/max $\Delta\rho$, e Å^{-3}	−1.886/1.955

114.52(4). Remaining C–C–C bond angles within the chain varies from 123.73(5) to 149.05(9) showing a corrugated organic chain structure with distortion throughout and having overall tilt angle of ∼45° (Fig. 1a). Here, the organic moiety is tagged to the iodides of two adjacent inorganic layers by terminal NH_3 groups *via* N–H–I hydrogen bonding with the three iodides (out of eight iodides) with a preference to terminal halide configuration: where the hydrogen bonding is with two terminal iodides and one bridging iodide (Fig. 1c). For comparison, in C12PI, the Pb–I distance varies from 3.183(2) Å to 3.200(2) Å. The *trans* Pb–I bond angle is 180° and the *cis* Pb–I bond angle vary from 86.16(3)° to 93.84(3)° and Pb–I–Pb bond angle is 150.59(4)°.

All the lead atoms in DDPI crystal are *in-plane* with perfect ordering because of less distortion in the I–Pb–I *cis* and *trans* angles which lead to more symmetrical geometry of PbI_6 octahedra layers (Fig. 1a). Whereas in C12PI, lead atoms are offset from layer to layer which resulted into more staggered arrangement of PbI_6 octahedra layers (Fig. 1b). Another interesting comparison is N–H–I bonding arrangement: bridging of N–H–I bonding in DDPI adopts "terminal halide" configuration of right triangle configuration while in C12PI the bridging adopts "equilateral configuration" (Fig. 1c and d). In DDPI a single organic is tagged in between two PbI planes with organic molecules bent by 45°, suggests comparatively more rigid nature of DDPI inorganic layers.

3.2. Physical and optical properties

Fig. 2a compares GLAXRD of DDPI thin film as well as powder pattern XRD. DDPI thin film show strong diffraction peak corresponding to the plane (1 0 0) at $2\theta = 5.58°$, followed by higher diffraction orders, related to (l 0 0) (l = 2, 3, 4,. . .), indicating well-stacked layered structure of DDPI. Both single crystal and thin films of DDPI show strong room-temperature excitonic features with symmetric and narrow line shape absorption at ∼510 nm and PL at ∼520 nm with full width half maximum (FWHM) of ∼11 nm (Fig. 2b). Extended Hückel tight-binding calculations [CAESAR^{TM} V2.0] [16] were used to evaluate band structure of the synthesized compound from the crystallographic structure data (Fig. 2c). Though this method underestimates the bandgap value, obtained value of ∼2.98 eV is in good agreement with the reported values of other 2D hybrids [11]. In general, the exciton energies are strongly dependent on several structural and physical properties of these hybrids. In these 2D layered IO-hybrids, band gap of organic layer (∼6 eV) is higher than inorganic layer (∼3 eV), therefore the excitons are tightly confined within the inorganic layers [6,17]. Recently, from the study of various mono-amino based IO-hybrids, apart from other important factors such as well/barrier widths, dielectric contrast etc., we have established a key relationship between the distortion of the inorganic (PbI) layers and the bandgap (and hence exciton energies) [11]. The results demonstrated that more PbI layer crumpling, i.e., decrease in Pb–I–Pb bond angle, results into increase of exciton peak energies. In this present work, room-temperature exciton PL of DDPI is observed at ∼520 nm, which is substantially higher than PL of C12PI (i.e. ∼500 nm), indicating that in DDPI, the PbI network is less crumpled. Even though Pb–I–Pb bond angle in DDPI (149.68°) is almost equal to that of C12PI (150.59°) (Fig. 1c and d), the PbI layered arrangement of DDPI, as seen from Fig. 1a and b (and the insets), suggests relatively less crumpled nature. The basic structural motif for all 2D IO-hybrids is the corner-sharing PbI_6 octahedra and the Pb–I–Pb bond angle brings out two kinds of distortions (i) the *out-of-plane* distortion which results into crumpling of layers and (ii) *in-plane* distortion which brings the PbI octahedra into closer proximity. Though *out-of-plane* distortion is most commonly observed in many mono-amino based IO-hybrids [8,11,18–20], in the present

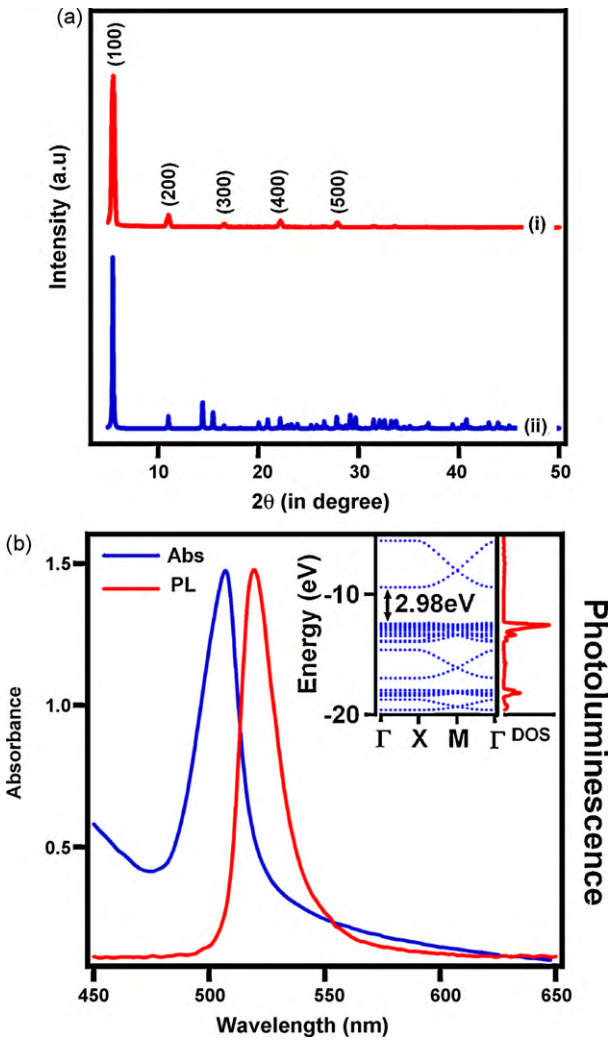

Fig. 2. (a) XRD patterns of (i) thin film and (ii) powder pattern obtained from single crystal XRD data. (b) Exciton absorption and emission spectra of DDPI thin film. Inset shows the band structure and corresponding density of states (DOS) of DDPI.

di-amino DDPI, both the distortions are to be considered. While Pb–I–Pb bond angle of DDPI appears closer to C12PI, the distortion in DDPI is predominantly *in-plane*, therefore less crumpling of PbI layers resulting into red-shifted PL energy.

We further experimented on alternate fabrication methods, such as intercalation process. Unlike the recently developed intercalation process [12], here we also fabricated DDPI crystals and thin films by reverse intercalation process, i.e., intercalating PbI_2 into the layered organic network. In this method, single crystals and thin films of organic (DD) were exposed to the solutions of PbI_2 dissolved in HI solvent. PL studies were performed on these intercalated films/crystals and are compared to the PL of conventionally prepared DDPI. Confocal microscopic image and the corresponding PL mapping of intercalated single crystal are shown in Fig. 3a and b respectively. PL spectral scans have been performed over an area of 1 mm^2 with 20 μm step size to study the surface morphology. To demonstrate the spectral variation, we have extracted PL spectra from the line scans, both *X* and *Y* directions of a particular location, and are presented in Fig. 3c. From these spectral line scans, it is clear that the PL line shape and position at various locations of intercalated single crystals are markedly different. Fig. 3d compares the PL spectra of conventional spin-coated film to the spectra of intercalated single crystal and thin films. As seen, while all PL spectra predominately indicating the DDPI phase, the spec-

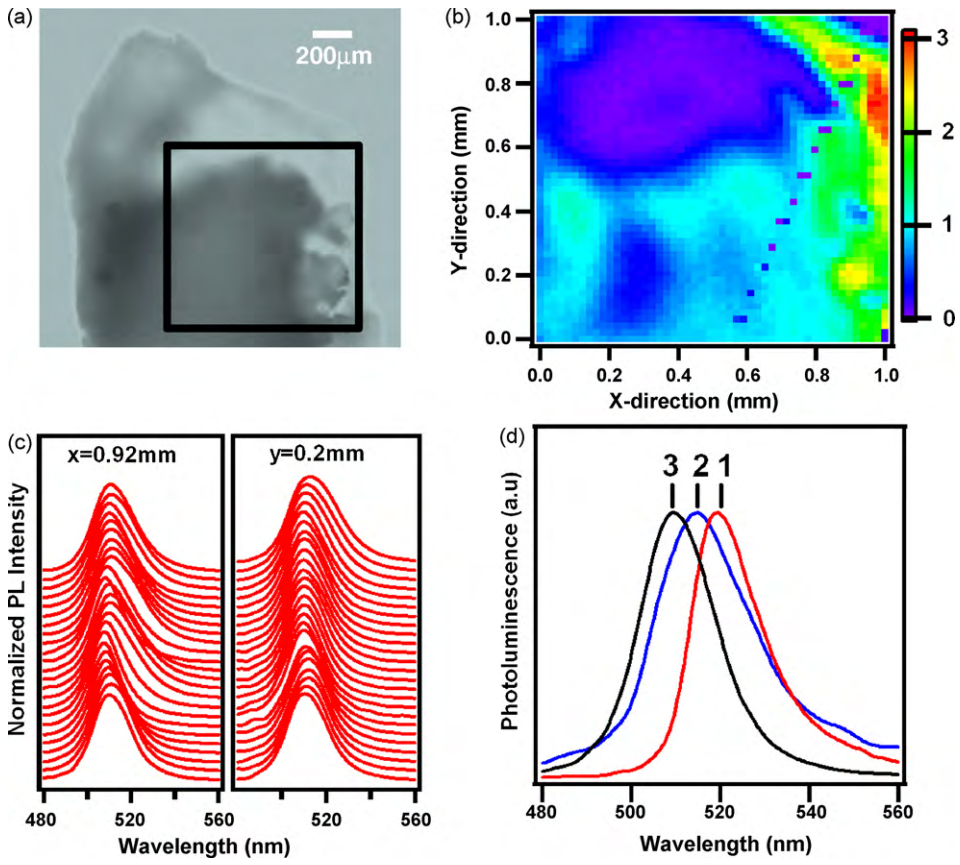

Fig. 3. (a) and (b) Confocal microscope image and PL intensity (at 510 nm) mapping of intercalated DDPI crystal. (c) Normalized PL spectra line scans along *y* and *x*-directions on the crystal shown in (b). Respective 'x' and 'y' locations are indicated in the figure and spectra are 'y' shifted for clarity. (d) The PL spectra of DDPI of different forms. 1, 2 and 3 indicate the PL spectra of conventional DDPI thin film, intercalated thin film and intercalated single crystals respectively.

tra of intercalated films and single crystals show about 10 nm blue shift than spin-coated films. Though further studies are required to fully understand the intercalation process, in our recent papers we have demonstrated that the optical characteristics of IO-hybrids are critically dependent on thickness and intercalation conditions. The heaviness of films and the presence of un-reacted entities may result into structural defects, such as imperfect lattice stacking of the PbI sheets and broken bonds within the PbI network, and as a consequence the perturbed exciton energy levels [2,10,11]. Therefore, the PL blue shift and broadness in intercalated films could be due to variation in PbI layering and film thickness [2,10–13]. For the same reason, the exciton PL line scans on various positions of intercalated single crystals (Fig. 3c) also show variation in peak position and intensity.

Supplementary data

Crystallographic data for the structure reported in this paper have been deposited with the Cambridge Crystallographic Data Centre as supplementary publication no. CCDC-750120. Copies of the data can be obtained free of charge on application to CCDC, 12 Union Road, Cambridge CB2 1EZ, UK (fax: +44 1223 336 033; e-mail: deposit@ccdc.cam.ac.uk).

Acknowledgements

Authors profoundly thank Prof. A. Ramanan, Department of Chemistry, IIT Delhi (India), and Prof. J.J. Baumberg, Cavendish Laboratory, Univ. of Cambridge (UK), for their help and encouragement. Also authors are thankful to Dr. R. Pallepogu, Univ. of Hyderabad (India), and Dr. M.E. Light, Univ. of Southampton (UK) for their technical help. One of the authors (GVP) acknowledges the financial support from DST, India. This work is part of *UK–India Education and Research Initiative* (UKIERI) programme.

References

[1] D.B. Mizi, K. Chondroudis, C.R. Kagan, IBM J. Res. Dev. 45 (2001) 29.
[2] G. Vijaya Prakash, K. Pradeesh, R. Ratnani, K. Saraswat, M.E. Light, J.J. Baumberg, J. Phys. D: Appl. Phys. 42 (2009) 185405.
[3] K. Pradeesh, M. Agarwal, K.K. Rao, G. Vijaya Prakash, Solid State Sci. 12 (2010) 95.
[4] G. Lanty, A. Bréhier, R. Parashkov, J.S. Lauret, E. Deleporte, New J. Phys. 10 (2008) 065007.
[5] Z. Cheng, B. Shi, B. Gao, M. Pang, S. Wang, Y. Han, J. Lin, Eur. J. Inorg. Chem. 1 (2005) 218.
[6] T. Ishihara, J. Takahashi, T. Goto, Phys. Rev. B 42 (1990) 11099.
[7] D.G. Billing, A. Lemmerer, Acta Cryst. Sec. B: Struct. Sci. B63 (2007) 735.
[8] D.G. Billing, A. Lemmerer, New J. Chem. 32 (2008) 1736.
[9] D.B. Mitzi, C.A. Field, W.T.A. Harrison, A.M. Guloy, Nature 369 (1994) 467.
[10] K. Pradeesh, J.J. Baumberg, G. Vijaya Prakash, Opt. Express 17 (2009) 22171.
[11] K. Pradeesh, J.J. Baumberg, G. Vijaya Prakash, Appl. Phys. Lett. 95 (2009) 173305.
[12] K. Pradeesh, J.J. Baumberg, G. Vijaya Prakash, Appl. Phys. Lett. 95 (2009) 033309.
[13] SMART & SAINT Software Reference Manuals, Version 6.22, Bruker AXS, Analytical Instrumentation, Madison, WI, USA, 2001.
[14] G.M. Sheldrick, SADABS, A Software for Empirical Absorption Correction, University of Gottingen, Gottingen, Germany, 2000.
[15] SHELXTL Reference Manual, Version 5.1, Bruker AXS, Analytical Instrumentation, Madison, WI, USA, 2000.
[16] Ren, W. Liang, M.-H. Whangbo, Crystal and Electronic Structure Analysis Using CAESAR, PrimeColor Software, Inc., USA, 1998, www.primec.com.
[17] E.A. Muljarov, S.G. Tikhodeev, N.A. Gippius, T. Ishihara, Phys. Rev. B 51 (1995) 14370.
[18] J.L. Knutson, J.D. Martin, D.B. Mitzi, Inorg. Chem. 44 (2005) 4699.
[19] Z. Xu, D.B. Mitzi, D.R. Medeiros, Inorg. Chem. 42 (2003) 1400.
[20] Z. Xu, D.B. Mitzi, C.D. Dimitrakopoulos, K.R. Maxcy, Inorg. Chem. 42 (2003) 2031.